

Exploring connections between global climate indices and African vegetation phenology

Molly E. Brown¹, Kirsten de Beurs², Anton Vrieling³

¹Biospheric Sciences Branch, NASA Goddard Space Flight Center, Greenbelt, MD 20771, United States

²Virginia Polytechnic Institute and State University, Department of Geography, 115 Major Williams Hall, Blacksburg, VA 24061, United States

³Joint Research Centre of the European Commission, TP266, Via E. Fermi 2749, 21027 Ispra (VA), Italy

Submitted to Remote Sensing of Environment, 3/2009

Abstract

Variations in agricultural production due to rainfall and temperature fluctuations are a primary cause of food insecurity on the continent in Africa. Agriculturally destructive droughts and floods are monitored from space using satellite remote sensing by organizations seeking to provide quantitative and predictive information about food security crises. Better knowledge on the relation between climate indices and food production may increase the use of these indices in famine early warning systems and climate outlook forums on the continent. Here we explore the relationship between phenology metrics derived from the 26 year AVHRR NDVI record and the North Atlantic Oscillation index (NAO), the Indian Ocean Dipole (IOD), the Pacific Decadal Oscillation (PDO), the Multivariate ENSO Index (MEI) and the Southern Oscillation Index (SOI). We explore spatial relationships between growing conditions as measured by the NDVI and the five climate indices in Eastern, Western and Southern Africa to determine the regions and periods when they have a significant impact. The focus is to provide a clear indication as to which climate index has the most impact on the three regions during the past quarter century. We found that the start of season and cumulative NDVI were significantly affected by variations in the climate indices. The particular climate index and the timing showing highest correlation depended heavily on the region examined. The research shows that climate indices can contribute to understanding growing season variability in Eastern, Western and Southern Africa.

1.0 Introduction

Satellite remote sensing has become a primary input to programs that monitor food production in Africa. In much of Africa, rainfed agriculture is a primary occupation and source of food for rural residents (Alberts and Mehta 2004; Breman 2003). Hundreds of millions of Africans rely on sufficient rainfall and moderate temperatures in order to produce enough food to feed their families (FAO 2006). Global trends in climate are increasingly impacting rainfall and temperature (Parry et al. 2007), which may ultimately reduce the ability of Africans to grow their own food (USAID 2007).

1
2 As population increases and food supplies become more constrained, the need to monitor
3 agricultural production even in the least productive regions will grow (Funk et al. 2008).
4 This highlights the need to understand the relationship between climate variability and
5 the indices that monitor local productivity. The amount of food produced locally often
6 interacts with global commodity prices to determine the price of food on the market,
7 affecting the ability of millions of poor urban and rural Africans to access food (Brown et
8 al. 2006). The stability of governments and regions often are disrupted when there is a
9 widespread lack of access and increasing hunger due to rising food prices (FEWS 2008;
10 Vasagar 2005).

11
12 Vegetation index data are often used by agencies monitoring agricultural conditions to
13 assess and predict agricultural production and identify periods of weather-related
14 production declines (Brown 2008b). Vegetation and rainfall data have become the basis
15 for operational monitoring of agricultural production, assessing variables such as the start
16 of season, growing season length and overall growing season productivity (Brown 2008a;
17 Brown and De Beurs 2008). Phenology metrics have a strong relationship with ultimate
18 food production, particularly those with sufficiently long records to capture local
19 variability (Funk and Budde 2008; Vrieling et al. 2008). Previous authors have used the
20 long term climate data record from the AVHRR instruments on the NOAA satellites as an
21 environmental observational record which may be directly related to climate variations
22 (Anyamba 1997; Verdin et al. 1999). Here we explore the relationship between
23 vegetation index data and five common climate indices to determine which most
24 influences local growing conditions in Sub-Saharan Africa.

25
26 Climate indices are used to reflect the essential elements of climate and its fluctuations
27 through time. ENSO (El Niño Southern Oscillation) is the best known index of climatic
28 variability, but others also express interannual climatic variability in Africa. Here we use
29 the North Atlantic Oscillation index (NAO), the Indian Ocean Dipole (IOD), the Pacific
30 Decadal Oscillation (PDO), the Multivariate ENSO Index (MEI) and the Southern
31 Oscillation Index (SOI). Each of these has been explored independently? in the literature
32 as to their impact on the African climate (Anyamba et al. 2001; Green and Hay 2002;
33 Jury et al. 1994; Rasmussen 1991; Verdin et al. 1999; Wang 2003). Strong negative SOI
34 anomalies are associated with an "El Niño" event (Cane et al. 1996) and strong positive
35 departures of the SOI are associated with "La Niña" conditions (Rasmusson and Wallace
36 1983). Warm ENSO events are characterized by above normal Sea Surface Temperatures
37 (SSTs) in the eastern Pacific and sometimes above normal SSTs in the western Indian
38 Ocean, as described by the IOD. Warm ENSO events, documented in the MEI, are
39 known to increase precipitation in some regions of Eastern Africa and result in droughts
40 in southern Africa (Glantz et al. 1991; Ropelewski and Halpert 1987).

41
42 By examining the spatial distribution and interaction of these effects, we can determine
43 which indices are most important in each region. This could provide guidance to model
44 developers and analysts working in the region. By conducting an analysis with many
45 climate indicators and multiple phenological metrics, we intend to cast a broad enough

1 net to provide guidance for data analysts who at present are focusing solely on one metric
2 in exclusion of others.

3 4 **2.0 Data**

5 6 **2.1 Normalized Difference Vegetation Index Data**

7 We used maximum value AVHRR NDVI composites (Holben 1986) from the NASA
8 Global Inventory Monitoring and Modeling Systems (GIMMS) group at NASA's
9 Biospheric Sciences Branch from July 1981 to December 2008 (Tucker et al. 2005). A
10 post-processing satellite drift correction has been applied to this dataset to further remove
11 artifacts due to orbital drift and changes in the sun-target-sensor geometry (Pinzon et al.
12 2005). The GIMMS operational dataset incorporates data from sensors aboard NOAA-7
13 through 14 with the data from the AVHRR on NOAA-16 and 17 using SPOT data as a
14 bridge for a by-pixel inter-calibration. Details of this calibration can be found in (Tucker
15 et al. 2005).

16 17 **2.2 Climate Indices**

18 We used five indices of global climate variations based on variations in atmospheric
19 pressure and sea surface temperatures from various regions. These are the North Atlantic
20 Oscillation index (NAO), the Indian Ocean Dipole (IOD), the Pacific Decadal Oscillation
21 (PDO), the Multivariate ENSO Index (MEI) and the Southern Oscillation Index (SOI).

22 We used the following indices:

- 23 • NAO: ftp://ftp.cpc.ncep.noaa.gov/wd52dg/data/indices/tele_index.nh
- 24 • IOD: <http://www.jamstec.go.jp/frsgc/research/d1/iod/>
- 25 • PDO: <http://jisao.washington.edu/pdo/PDO.latest>
- 26 • MEI: <http://www.cdc.noaa.gov/ClimateIndices/>
- 27 • SOI: <http://www.cpc.ncep.noaa.gov/data/indices/soi>

28 Figure 1 gives an overview of the variability of the indices over the past 26 years.

29 A mode of climate variability with extensive effects in the Northern Hemisphere, is the
30 Northern Annular Mode (NAM; (Thompson and Wallace 2001)), which also goes by the
31 name of the North Atlantic Oscillation (NAO; (Hurrell 1995)). The North Atlantic
32 Oscillation (NAO) index is typically measured through variations in the normal pattern of
33 lower atmospheric pressure over Iceland and higher pressure near the Azores and Iberian
34 Peninsula (Jones et al. 1997). A positive NAO index refers to an increased difference in
35 pressure between these two regions and thus stronger westerly winds. This corresponds to
36 a stronger storm track across the Atlantic from Western Africa. The negative mode of the
37 NAO—when there is less difference than usual in pressure across the two regions—
38 features a weakened Atlantic storm track. The NAO trended toward more positive values
39 from the 1960s to the mid-1990s, but has since returned to more normal values (UCAR
40 2009).

41 The Indian Ocean Dipole (IOD) is an interannual (year-to-year) climate pattern across the
42 tropical Indian Ocean first identified in 1999 (Saji et al. 1999). In the positive phase of
43 the IOD, trade winds are stronger than usual and cooler-than-average sea-surface
44 temperatures are prevalent across the eastern tropical Indian Ocean, near Indonesia and

1 Australia. To the west, near Madagascar, waters are warmer than average and convection
2 is intensified, thus causing heavy rainfall in Eastern parts of Africa. These patterns are
3 reversed during the IOD's negative phase(UCAR 2009).

4
5 The Pacific Decadal Oscillation (PDO) is a multidecadal pattern of climate variability
6 centered across the North Pacific Ocean (Mantua et al. 1997). During the positive (warm)
7 phase of the PDO, sea-surface temperatures tend to be above average along the west
8 coast of North America and in the eastern tropical Pacific; while across the central North
9 Pacific they are cooler than average. The opposite patterns occur during the negative
10 (cool) phase. The PDO may be related to ENSO, but differs mainly because the timescale
11 for the PDO is much longer (several decades) and because the PDO more clearly involves
12 the extratropical Pacific and the Aleutian low pressure system (UCAR 2009). The
13 impact of the PDO on the climate of Africa during the past few decades is unclear,
14 although studies suggest a correlation with rainfall in Eastern and Southern Africa
15 (Mantua and Hare, 2002).

16
17 The Multivariate ENSO Index (MEI) is a measure of the comparative strength of El Nino
18 Southern Oscillation (ENSO) events (Wolter and Timlin 1998). It is derived by
19 combining several different indices that separately measure weather variables in the
20 tropical Pacific, such as sea-surface temperature, sea-level pressure (SOI), surface winds,
21 surface air temperature, cloudiness, precipitation, and other variables (UCAR 2009).

22
23 Finally, the Southern Oscillation Index (SOI) is a measure that represents the strength of
24 the Southern Oscillation in the Pacific Ocean sea surface temperatures and pressures
25 (Reynolds et al. 2002). An SOI is typically created by comparing the sea-level pressures
26 measured at Tahiti (in the South Pacific) to those at Darwin, Australia, and listing the
27 anomalies (the departures from average). During El Niño, pressures tend to be below
28 normal at Tahiti and above normal at Darwin, producing a negative SOI. The opposite is
29 true during La Niña (UCAR 2009). Research has shown that negative SOI (El Niño) is
30 associated with dry weather and a positive SOI (La Niña) related to wet weather
31 conditions in Southern Africa. These variations are linked to variations in malaria
32 incidence (Mabaso et al. 2009).

34 **3.0 Methods**

35
36 The NDVI data were temporally filtered and phenology parameters were extracted in
37 order to estimate the potential impact of the climate indices on growing season variability
38 in the region and consequently on food production. Temporal filtering was performed to
39 reduce any remaining cloud effect in the NDVI data by means of an iterative Savitzky-
40 Golay filter (Chen et al. 2004). Three regions were analyzed, Eastern Africa, Western
41 Africa and Southern Africa (Figure 2).

42
43 To extract phenology variables, we used the percent threshold or mid-point NDVI
44 method proposed by (White et al. 1997). The onset and conclusion of the growing season
45 are estimated using NDVI curves, extracting for each pixel and year the start of season
46 (SOS), and end of season (EOS) as the timing of the crossing of the 50% point of the

1 NDVI curve in upward or downward direction respectively. Since the African growing
2 seasons do not everywhere fall within one calendar year, we determined SOS and EOS
3 based on two different time periods both incorporating 1.5 years of data: Cycle 1:
4 October Year 1 – March Year 3 Cycle 2: April Year 2 – October Year 3 (Figure 3).
5 These time frames allow for the estimation of growing seasons in both the Northern
6 Hemispheric and the Southern Hemispheric parts of Africa. In addition, it allows for the
7 detection of double cropped regions such as can be found in Eastern Africa.

8
9 A total of five phenology indicators were considered for this analysis. Besides SOS and
10 EOS, we determined the length of season (LOS), the maximum NDVI of the season
11 (maxNDVI), and the cumulated NDVI over the season (cumNDVI). The extraction of
12 these parameters is straightforward based on SOS, EOS, and the filtered time series
13 (Figure 4). The length of season (LOS) parameter is calculated as $LOS = EOS - SOS$. We
14 defined that LOS should be at least more than a month to be valid, and before calculating
15 other indicators.

16
17 The five phenology indicators described above were correlated to the five climate
18 indices NAO, PDO, MEI, IOD and SOI. To reduce noise and increase the signal for each
19 climate index, we aggregated the monthly data into four seasons to determine the
20 correlation with the vegetation index phenology indicators: DJF – December, January,
21 February; MAM – March, April, May; JJA – June, July, August; and SON – September,
22 October, November. These were then correlated with the annual phenology indicators
23 over two-year cycles to capture the effect of the index during each season on the annual
24 phenology metrics for the same year as the index aggregation and on the next year,
25 enabling the capturing of as broad a range of impact as possible of each climate indicator.

26
27 We used the non-parametric Spearman rank correlation to determine the strength of the
28 association between the climate indices and the phenological metrics (Lehman and
29 D'Abbrera 1975). The Spearman rank correlation coefficient is based on the ranked values
30 of the variables rather than on the values themselves as in the common Pearson
31 correlation coefficient. The Spearman correlation makes no assumption with respect to
32 the underlying frequency of the variables and does not presume the variables to be
33 linearly related. Since theoretical studies have shown that the interaction between
34 vegetation and atmosphere is non-linear, e.g. (Bonan 2002), these are important
35 considerations. If the interaction were indeed non-linear, the Pearson correlation
36 coefficient or simple linear regression could either over or under estimate the strength of
37 the relation (de Beurs and Henebry 2008).

38
39 The results were simplified into the three regions of interest where the NDVI has the
40 strongest correlation to production in semi-arid zones: Eastern, Southern and Western
41 Africa. We calculated the total number of pixels with positive and with negative trend
42 correlations in the regions as well as the percent of significant trends within each
43 category (Figure 5). In this way we were able to characterize the overall impact of a
44 particular climate index for a region and therefore its importance on growing conditions
45 during the past 26 years.

46

1 When a statistical test (such as the Spearman rank correlation test) is run a large number
2 of times, a certain number of false positive results is expected. The rate of false positives
3 allowed for the test statistic is determined by the α -level. For example, if we set the α -
4 level at 0.10 and we apply a statistical test 1000 times, we could expect to find about 100
5 rejections of the null hypothesis while there is in fact no correlation (de Beurs and
6 Henebry 2008). Here we analyze the correlation results by region. By setting our α -level
7 at 0.10, we argue that a geographic region with more than the expected 10% significant
8 pixels, can be considered to have revealed significant correlation. We report our findings
9 using the percent of the geographic area with either positive or negative significant
10 correlations between SOS and CumNDVI and the climate index in a season in the interest
11 of space. The influence of the climate indicator is thus estimated using vegetation index
12 data from the past 25 years, estimating its impact on the local climate and agricultural
13 production across a broad region. In the next section we will present the key findings.

14 **4.0 Results**

15 **4.1 Regional Results**

16
17
18
19 In Southern Africa we found that all climate indices were influential on one or more of
20 the phenology parameters at some period of the year. As other authors have found,
21 Southern Africa is sensitive to both the pacific and ENSO effects (Eastman et al. 1996;
22 Nicholson 2003; Ropelewski and Halpert 1986). The end of the growing season
23 parameter was particularly sensitive to the PDO, MEI, NAO and IOD, although this
24 parameter may be less robust than that of SOS or the cumulative NDVI (detailed below).

25
26 Eastern Africa, with results from both cycle 1 and cycle 2 analyses, the SOS shows a
27 sensitivity to the PDO indicator during the MAM and DJF periods, with less impact at
28 other times of the year. The MEI index also has a very strong influence on SOS and
29 CumNDVI in the region, particularly in SON and DJF. NAO and IOD have only a small
30 influence in the region.

31
32 In Western Africa, PDO was the most important index, influencing both the start and
33 length of the growing season in the central area comprising northern Nigeria, Ghana
34 and the Ivory Coast. The two ENSO indicators MEI and SOI also have their impact in
35 the growing season, but the effect is less strong than the PDO. The NAO during SON
36 had a strong negative influence on the start of season (e.g. 61% of Western Africa
37 revealed a positive correlation between SOS and NAO_SON0, which is the September-
38 October-November period preceding the observed growing season, Table 1), end of
39 season and the season length (Fontaine et al. 1998). The IOD did not seem to have much
40 influence in the region.

41 **4.2 Start of Season Results**

42
43
44 SOS is an important measure of the ultimate success of the growing season in many
45 rainfed agricultural systems (Brown and De Beurs 2008; Funk and Budde 2008).
46 Delayed starts shorten the growing season in some regions, directly reducing the yield

1 because generally the rains end before crops are fully mature. In other regions, variations
2 in global climate indices are related to early starts, which may provide a longer season
3 with more rain.

4
5 Table 1 reports the impact of each climatic index on SOS from eight different three
6 month groups. The climate indices start three 3-month periods before the growing season
7 e.g. for Southern Africa and the second cycle of Eastern Africa the growing season
8 typically starts in the period September-October-November (the *belg* rains in Ethiopia).
9 NAO-DJF1 is the NAO index of December-January-February in the year 1, thus three 3-
10 month periods before average SOS in Southern and Eastern Africa. The growing season
11 in Western Africa and the first cycle of Eastern Africa typically starts in the period
12 March-April-May of year 1 (MAM1). The correlations are reported for the indices
13 starting three 3-month periods earlier (e.g. June-July-August of year 0).

14
15 The results show that in the first growing cycle in Eastern Africa, the March-April-May
16 Pacific Decadal Oscillation (PDO_MAM1) affects the start of the growing season in 72%
17 of the region with a positive correlation, meaning when the PDO is elevated, the growing
18 season will start later in 72% of the region. This correlation is significant in 32% of the
19 region. It is interesting to see that the two preceding periods (PDO_SON0 and
20 PDO_DJF1) also reveal between 70-72% positive correlation between SOS and PDO.
21 However, the correlation is significant in a lower percentage of pixels (18 and 24%
22 respectively).

23
24 Figure 5 shows the spatial distribution of the correlation between SOS and PDO_MAM1
25 with their corresponding p-values. A large area of positive significant correlation can be
26 seen in Eastern Ethiopia as well as on the border between Ethiopia and Sudan, the site of
27 an ongoing and severe drought. There is another area with significant positive correlation
28 in central Kenya. It is interesting to see north-south patch of significant negative
29 correlation in the higher laying areas of central Ethiopia. Eastern Africa also reveals
30 positive correlation in 72% of the region between the Multivariate ENSO Index (MEI)
31 during the DJF period (MEI_DJF1) and the start of the growing season in Eastern Africa.
32 Again, the two preceding periods (MEI_JJA0 and MEI_SON0) reveal similar positive
33 correlation. This time the percentage of significant correlations is about 18% for all three
34 time periods. Correlations with SOI are reversed, with 75% negative correlation between
35 SOS and SOI_JJA0.

36
37 Southern African phenology metrics are influenced by from all five climate metrics. The
38 SOI index shows positive correlations with changes in SOS, and NAO, PDO, and IOD
39 reveal negative correlations with the start of season (Table 1). MEI reveals both positive
40 and negative correlations, although at different timings. Figure 6A and 6B shows the
41 impact on the start of the growing season in Southern Africa of the Multivariate ENSO
42 Index from March-April-May (MAM-1). This is two periods before average SOS in
43 Southern Africa which falls between September and November. The region reveals
44 positive correlation in 71% of the pixels, with 20% of the pixels being significant.

45

1 Figure 6 C and D show the correlation between IOD from June-July-August on the start
2 of season (SOS) in Southern Africa. This is one period before the season starts in
3 Southern Africa. In this case 71% of the region reveals positive correlation (19% is
4 significant). Note the spatial pattern of the significance, with strong correlation and
5 significance in the dryland regions of central Mozambique and eastern Zimbabwe,
6 regions with fairly marginal agricultural productivity but with high variability from year
7 to year. Also, the border area between Namibia, Botswana and South Africa reveals a
8 region of with IOD significant negative correlation.

9
10 In Western Africa, the correlation patterns are generally less uniform, resulting in a
11 mixture of positive and negative correlations. As a result, the regional percentage of
12 correlation that is either positive or negative is lower. The Pacific Decadal Oscillation
13 (PDO_DJF1) reveals one of the few significant positive correlations with the SOS
14 (percentage positive is 0.66), as is seen in Table 1 and in Figure 7. The correlation
15 between the December-January-February values of the PDO on SOS in the northern parts
16 of Ivory Coast, Nigeria and central Guinea Conakry mean that when the PDO is elevated,
17 the start of season is later.

18 19 **4.3 Cumulative NDVI results**

20
21 Cumulative NDVI has long been a parameter which has been used to correspond to
22 growing period, agricultural productivity, changes in landscape pattern and other
23 parameters (Chen et al. 2000; Chuvieco 1999; Ji and Peters 2003; Rasmussen 1998).
24 Figure 8A shows the correlation between the MEI from September-October-November
25 (MEI_SON1) on cumulative NDVI from Cycle 2 (long season rains) in Eastern Africa
26 (75% positive correlation). Figure 8B shows the significance (p-value, 22% significant).
27 This period coincides with SOS for the second cycle in Eastern Africa. The next two 3-
28 month period, which fall within the growing season, also reveal high percentages of
29 significant positive correlations. Figure 8C shows the correlation between the SOI from
30 June-July-August (SOI_JJA1) on cumulative NDVI and Figure 8D the significance of the
31 correlation. SOI values in June-July-August (SOI_JJA1) show significant (75% of the
32 pixels are negatively correlated, 31% of the correlations are significant) and strong
33 correlations with cumulative NDVI in the eastern and central Ethiopia and the rangeland
34 areas of Kenya (Figure 8). Again, the two preceding periods which still fall within the
35 growing season, show similar significant correlations. These spatial patterns are very
36 interesting given the long term drought seen in these regions during the past few years.

37
38 Table 2 highlights the strong relationship between PDO and the cumulative NDVI in
39 Western Africa before the actual start of the growing season. PDO reveals significant
40 negative correlations with cumulative NDVI in the four periods JJA0, SON0, DJF1 and
41 MAM1. The growing season typically starts during the period MAM1. The regions where
42 strong PDO relationships are seen for the cumulative NDVI are similar to those seen for
43 SOS (Figure 7), which is to be expected since a delayed start of season will result in a
44 lower cumulative NDVI.

45 46 **4.4 Results by region, with a focus on the Pacific Decadal Oscillation**

1
2 Figure 9 shows plots for each region that summarize the effect of four parameters on SOS
3 in each region. For clarity we have omitted SOI, which shows a similar although opposite
4 pattern as MEI. The figures show the percent of the region with negative correlations
5 between the climate index and SOS. Negative correlations denote an earlier SOS for a
6 higher index value. Only the values for the second cycle of Eastern Africa are plotted.
7 Note the strong negative correlations between SOS and PDO in both Eastern and
8 Southern Africa, more than 70% of the region affected. The area that the PDO influences
9 grows through time, with stronger correlations during the growing season than in the dry
10 season. In both Southern and Eastern Africa the climate indices appear to become fairly
11 similar around the time of SOS (indicated by the vertical line).
12

13 Figure 10 shows the results for all three regions divided by climatic index. Figure 10A
14 shows the results for the PDO and are particularly interesting. In both Southern and
15 Western Africa, the index is revealing strong correlations, with high negative correlation
16 in Western Africa and high positive (thus low negative) correlation in Southern Africa.
17 The impact of the PDO on the climate of Africa during the past few decades is unclear,
18 although Rouault (2002) examined the association between the PDO and South African
19 rainfall and noted that the warm (cool) phase of the interdecadal variability in the Pacific
20 and Indian Ocean is associated with decreased (increased) rainfall over South Africa
21 (Reason and Rouault 2002). Figure 10B shows the MEI and 10C the NAO results. The
22 MEI has the strongest seasonal effect, increasing during the short and long seasons of
23 Eastern Africa and declining since.
24

25 **5.0 Discussion**

26
27 The results of this paper highlight climate-vegetation relationships that could be very
28 valuable for the analysis of seasonal variation in the climate in Africa. The relationships
29 we find here are evidence of recurring and persistent, large-scale pattern of pressure and
30 circulation anomalies that span vast geographical areas. Here we show that seasonal
31 phenological patterns as derived from the 26 year vegetation index record can be used to
32 estimate the importance or lack of importance of the various indices in Western, Eastern
33 and Southern Africa.
34

35 The GIMMS NDVI dataset is not perfect as a source of information on agricultural
36 productivity or characteristics. Here we transform the bimonthly dataset into five
37 phenological parameters, but these are not equal in stability. Previous research and
38 extensive use of GIMMS NDVI and phenology metrics in Africa through the USAID's
39 Famine Early Warning Systems Network has shown that the start of season and
40 cumulative NDVI are the most stable and reliable parameters, with the longest record of
41 use and publications in Africa (Brown 2008b). The end of season parameter is influenced
42 by land cover type and the cumulative NDVI could be affected by the degree of
43 cloudiness during the peak of the rainy season and the calibration between sensors
44 through time (Tucker et al. 2005). However, by using phenological parameters, we are
45 able to move significantly closer to understanding the impact of climate variability on
46 agriculture.

1
2 SOS is particularly important for determining yields in a given season, since in many
3 semi-arid areas, the length of the growing season is an important determinant of yield. If
4 the season begins late, the likelihood of average yields declines significantly (FEWS
5 1992; Groten and Ocatre 2002; Verdin et al. 2000). Thus negative correlations (implying
6 a later start for lower index values) with SOS over the 25 year NDVI record is an
7 important estimate of the impact of the climate indicator on overall agricultural
8 productivity in that season because in semi-arid zones, a delayed start results in reduced
9 yields. Variations in climate indices can then be used to estimate future changes in
10 growing season length, start and strength based on this research.

11
12 In Eastern Africa, we found high negative correlations between SOS during the second
13 cycle and MEI, particularly in the semi-arid pastoral zone of eastern Ethiopia, Somalia
14 and northeastern Kenya (see Figure 8). This region has been experiencing a multi-year
15 drought during the past decade which has resulted in failed harvests, water shortages and
16 deteriorating rangeland conditions (FEWSNET 2006; Funk et al. 2005). The effect of the
17 global climate system on this region where there are millions of food insecure and hungry
18 agriculturalists and pastoralists has been a topic of much recent research (Funk et al.
19 2008)

20
21 In Western Africa, we have identified a similar relationship between the Atlantic
22 multidecadal variability as represented by the NAO and Sahel rainfall as was documented
23 in (Zhang and Delworth 2006). Exploration of these relationships in the context of
24 prediction and estimation of rainfall in the region is warranted, and may result in
25 improved seasonal prediction in, for example, the regional climate outlook forums held
26 before the main growing season every year (Brown et al. 2007).

27
28 Future research will focus on the forecasting potential of climatic indices for
29 phenological metrics and thus crop production. Future steps would be to assess the
30 simultaneous impact of multiple climatic indices on the observed phenology events.
31 Impacts of different indices could be additive, potentially resulting in increased
32 explanatory power. In addition, our figures show that high correlation exists in sub-
33 regions of Western, Eastern and Southern Africa. Thus, detailed impact studies in sub-
34 regions may be useful as well.

35 36 **6.0 Conclusions**

37
38 Given the agricultural nature of most economies on the African continent, agricultural
39 production continues to be a critical determinant of both food security and economic
40 growth (Funk and Brown 2009). In this paper, we explore the relationship between
41 climate indices and phenology metrics derived from NDVI data to determine how
42 influential each metric is on the growing season. Crop phenological parameters, such as
43 the start and end of the growing season, the total length of the growing season, and the
44 rate of greening and senescence are important for planning crop management and crop
45 diversification and intensification. Because these crop parameters are sensitive to climate
46 variability, understanding which climate indices are most influential and affect variation

1 in these metrics from one year to the next can improve seasonal analysis and agriculture
2 planning across the continent.

3

4 We found that the start of season and cumulative NDVI were significantly affected by
5 variations in the climate indices in the three regions examined. Eastern Africa that has
6 been experiencing drought in recent years is particularly sensitive to PDO variations in
7 March-April-May. In Western Africa, we have identified a relationship between NAO
8 and Sahel rainfall as expressed by vegetation. The growing season in Southern African is
9 sensitive to variations in the ENSO metrics SOI and MEI, as well as PDO. Research that
10 uses current climate indices to estimate variability in the next growing season for each
11 region is the subject of future research, as this will enhance the utility of this research for
12 many users of remote sensing in the region.

Table 1. Start of Season correlation and significance for five metrics and three regions. %+ = the percentage of pixels with positive correlation. %+ sig = the percentage of pixels with positive correlation that are significant. %- = the percentage of pixels with negative correlation. %-sig = percentage of pixels with negative correlation that are significant. Eastern Africa results are from Cycle 1 results, derived from the January to December period.

<i>Index</i>	<i>Southern Africa</i>				<i>Eastern Africa</i>				<i>Western Africa</i>				
Period	%+	%+ sig.	%-	%-sig.	%+	%+ sig.	%-	%-sig.	%+	%+ sig.	%-	%-sig.	Period
	←	←	←	←	←	←	←	←	←	←	←	←	
	→	→	→	→	→	→	→	→	→	→	→	→	
NAO_DJF1	0.51	0.09	0.49	0.08	0.43	0.10	0.57	0.10	0.34	0.05	0.66	0.13	NAO_JJA0
NAO_MAM1	0.33	0.04	0.67	0.13	0.44	0.05	0.56	0.10	0.61	0.14	0.39	0.08	NAO_SON0
NAO_JJA1	0.69	0.16	0.31	0.04	0.59	0.09	0.41	0.06	0.43	0.07	0.57	0.11	NAO_DJF1
NAO_SON1	0.29	0.09	0.71	0.23	0.44	0.06	0.56	0.08	0.45	0.05	0.55	0.08	NAO_MAM1
NAO_DJF2	0.51	0.08	0.49	0.07	0.34	0.07	0.66	0.16	0.53	0.07	0.47	0.06	NAO_JJA1
NAO_MAM2	0.49	0.11	0.51	0.09	0.40	0.05	0.60	0.10	0.39	0.06	0.61	0.13	NAO_SON1
NAO_JJA2	0.53	0.08	0.47	0.07	0.50	0.08	0.50	0.08	0.52	0.09	0.48	0.07	NAO_DJF2
NAO_SON2	0.49	0.11	0.51	0.13	0.31	0.04	0.69	0.16	0.57	0.15	0.43	0.14	NAO_MAM2
PDO_DJF1	0.36	0.05	0.64	0.11	0.56	0.08	0.44	0.09	0.49	0.06	0.51	0.07	PDO_JJA0
PDO_MAM1	0.45	0.06	0.55	0.10	0.72	0.18	0.28	0.04	0.59	0.10	0.41	0.05	PDO_SON0
PDO_JJA1	0.60	0.10	0.40	0.06	0.70	0.24	0.30	0.10	0.66	0.17	0.34	0.05	PDO_DJF1
PDO_SON1	0.32	0.04	0.68	0.15	0.72	0.32	0.28	0.11	0.57	0.13	0.43	0.06	PDO_MAM1
PDO_DJF2	0.24	0.03	0.76	0.18	0.56	0.13	0.44	0.09	0.48	0.07	0.52	0.09	PDO_JJA1
PDO_MAM2	0.28	0.04	0.72	0.14	0.56	0.14	0.44	0.08	0.43	0.07	0.57	0.11	PDO_SON1
PDO_JJA2	0.40	0.06	0.60	0.08	0.61	0.16	0.38	0.13	0.53	0.10	0.47	0.07	PDO_DJF2
PDO_SON2	0.43	0.09	0.57	0.10	0.50	0.10	0.50	0.11	0.40	0.06	0.60	0.10	PDO_MAM2
MEI_DJF1	0.67	0.14	0.33	0.05	0.73	0.18	0.27	0.04	0.55	0.07	0.45	0.05	MEI_JJA0
MEI_MAM1	0.71	0.20	0.29	0.05	0.72	0.17	0.28	0.04	0.61	0.12	0.39	0.08	MEI_SON0
MEI_JJA1	0.38	0.08	0.62	0.15	0.72	0.18	0.28	0.04	0.59	0.13	0.41	0.08	MEI_DJF1
MEI_SON1	0.27	0.06	0.73	0.20	0.60	0.14	0.40	0.09	0.50	0.12	0.50	0.13	MEI_MAM1
MEI_DJF2	0.29	0.07	0.71	0.20	0.57	0.14	0.43	0.08	0.38	0.11	0.62	0.17	MEI_JJA1
MEI_MAM2	0.38	0.08	0.62	0.15	0.52	0.12	0.48	0.09	0.36	0.07	0.64	0.14	MEI_SON1
MEI_JJA2	0.43	0.11	0.57	0.11	0.44	0.08	0.56	0.11	0.35	0.08	0.65	0.14	MEI_DJF2
MEI_SON2	0.50	0.10	0.50	0.08	0.32	0.06	0.68	0.19	0.25	0.04	0.75	0.22	MEI_MAM2

IOD_DJF1	0.52	0.08	0.48	0.07	0.73	0.17	0.27	0.04	0.60	0.13	0.40	0.05	IOD_JJA0
IOD_MAM1	0.39	0.08	0.61	0.17	0.75	0.16	0.25	0.03	0.60	0.14	0.40	0.08	IOD_SON0
IOD_JJA1	0.29	0.05	0.71	0.19	0.63	0.12	0.37	0.05	0.64	0.10	0.36	0.05	IOD_DJF1
IOD_SON1	0.32	0.05	0.68	0.16	0.60	0.11	0.40	0.05	0.45	0.08	0.55	0.10	IOD_MAM1
IOD_DJF2	0.43	0.06	0.57	0.09	0.60	0.11	0.40	0.06	0.47	0.06	0.53	0.11	IOD_JJA1
IOD_MAM2	0.54	0.07	0.46	0.06	0.52	0.08	0.48	0.07	0.52	0.07	0.48	0.08	IOD_SON1
IOD_JJA2	0.43	0.07	0.57	0.08	0.47	0.07	0.53	0.09	0.64	0.13	0.36	0.06	IOD_DJF2
IOD_SON2	0.49	0.07	0.51	0.06	0.36	0.04	0.64	0.11	0.53	0.09	0.47	0.08	IOD_MAM2
SOI_DJF1	0.32	0.05	0.68	0.15	0.25	0.04	0.75	0.17	0.35	0.04	0.65	0.12	SOI_JJA0
SOI_MAM1	0.40	0.07	0.60	0.15	0.30	0.06	0.70	0.17	0.44	0.08	0.56	0.11	SOI_SON0
SOI_JJA1	0.69	0.17	0.31	0.05	0.34	0.06	0.66	0.15	0.36	0.07	0.64	0.14	SOI_DJF1
SOI_SON1	0.69	0.17	0.31	0.06	0.39	0.09	0.61	0.19	0.54	0.15	0.46	0.12	SOI_MAM1
SOI_DJF2	0.74	0.22	0.26	0.05	0.39	0.06	0.61	0.12	0.61	0.15	0.39	0.07	SOI_JJA1
SOI_MAM2	0.62	0.17	0.38	0.09	0.59	0.11	0.40	0.07	0.68	0.17	0.32	0.08	SOI_SON1
SOI_JJA2	0.51	0.07	0.49	0.10	0.62	0.14	0.38	0.07	0.69	0.15	0.31	0.04	SOI_DJF2
SOI_SON2	0.44	0.07	0.56	0.13	0.70	0.16	0.30	0.07	0.73	0.23	0.27	0.09	SOI_MAM2

Table 2. Cumulative NDVI correlation and significance for five metrics and three regions. %+ = the percentage of pixels with positive correlation. %+ sig = the percentage of pixels with positive correlation that are significant. %- = the percentage of pixels with negative correlation. %-sig = percentage of pixels with negative correlation that are significant. The Western Africa percentages use the index labels on the right.

<i>Index</i>	<i>Southern Africa</i>				<i>Eastern Africa</i>				<i>Western Africa</i>				
Period	%+	%+ sig.	%-	%-sig.	%+	%+ sig.	%-	%-sig.	%+	%+ sig.	%-	%-sig.	Period
	←	←	←	←	←	←	←	←	←	←	←	←	→
NAO_DJF1	0.44	0.08	0.56	0.11	0.40	0.06	0.60	0.12	0.37	0.07	0.63	0.14	NAO_JJA0
NAO_MAM1	0.45	0.07	0.55	0.09	0.70	0.17	0.30	0.05	0.36	0.05	0.64	0.11	NAO_SON0
NAO_JJA1	0.54	0.10	0.46	0.07	0.48	0.08	0.52	0.08	0.52	0.06	0.48	0.06	NAO_DJF1
NAO_SON1	0.38	0.06	0.62	0.15	0.48	0.07	0.52	0.07	0.54	0.08	0.46	0.06	NAO_MAM1
NAO_DJF2	0.45	0.07	0.55	0.11	0.36	0.04	0.64	0.12	0.41	0.06	0.59	0.07	NAO_JJA1
NAO_MAM2	0.41	0.07	0.59	0.11	0.31	0.05	0.69	0.22	0.36	0.07	0.64	0.13	NAO_SON1
NAO_JJA2	0.27	0.04	0.73	0.18	0.28	0.04	0.72	0.15	0.47	0.09	0.53	0.08	NAO_DJF2
NAO_SON2	0.58	0.16	0.42	0.11	0.50	0.09	0.50	0.09	0.43	0.11	0.57	0.15	NAO_MAM2
PDO_DJF1	0.56	0.12	0.44	0.09	0.44	0.07	0.56	0.10	0.27	0.06	0.73	0.21	PDO_JJA0
PDO_MAM1	0.52	0.08	0.48	0.08	0.40	0.09	0.60	0.13	0.30	0.05	0.70	0.17	PDO_SON0
PDO_JJA1	0.60	0.09	0.40	0.05	0.62	0.10	0.38	0.05	0.30	0.05	0.70	0.18	PDO_DJF1
PDO_SON1	0.33	0.05	0.67	0.12	0.65	0.12	0.35	0.05	0.30	0.04	0.70	0.15	PDO_MAM1
PDO_DJF2	0.42	0.07	0.58	0.10	0.59	0.10	0.41	0.06	0.39	0.06	0.61	0.08	PDO_JJA1
PDO_MAM2	0.39	0.06	0.61	0.11	0.59	0.11	0.41	0.07	0.35	0.12	0.65	0.25	PDO_SON1
PDO_JJA2	0.33	0.06	0.67	0.14	0.50	0.07	0.50	0.08	0.33	0.10	0.67	0.20	PDO_DJF2
PDO_SON2	0.44	0.07	0.56	0.09	0.45	0.08	0.55	0.09	0.38	0.07	0.62	0.10	PDO_MAM2
MEI_DJF1	0.42	0.06	0.58	0.10	0.28	0.04	0.72	0.15	0.37	0.07	0.63	0.12	MEI_JJA0
MEI_MAM1	0.43	0.05	0.57	0.09	0.37	0.06	0.63	0.12	0.29	0.07	0.71	0.16	MEI_SON0
MEI_JJA1	0.35	0.08	0.65	0.17	0.66	0.13	0.34	0.06	0.33	0.06	0.67	0.14	MEI_DJF1
MEI_SON1	0.33	0.07	0.67	0.18	0.75	0.22	0.25	0.05	0.37	0.05	0.63	0.14	MEI_MAM1
MEI_DJF2	0.33	0.08	0.67	0.21	0.74	0.25	0.26	0.06	0.44	0.07	0.56	0.12	MEI_JJA1
MEI_MAM2	0.30	0.08	0.70	0.25	0.72	0.24	0.28	0.07	0.40	0.06	0.60	0.10	MEI_SON1
MEI_JJA2	0.33	0.06	0.67	0.18	0.51	0.08	0.49	0.08	0.47	0.08	0.53	0.09	MEI_DJF2
MEI_SON2	0.36	0.05	0.64	0.13	0.32	0.05	0.68	0.15	0.53	0.11	0.47	0.10	MEI_MAM2

IOD_DJF1	0.33	0.05	0.67	0.13	0.42	0.06	0.58	0.10	0.47	0.07	0.53	0.09	IOD_JJA0
IOD_MAM1	0.39	0.06	0.61	0.11	0.49	0.08	0.51	0.08	0.37	0.05	0.63	0.12	IOD_SON0
IOD_JJA1	0.35	0.05	0.65	0.12	0.57	0.10	0.43	0.08	0.41	0.05	0.59	0.08	IOD_DJF1
IOD_SON1	0.44	0.07	0.56	0.10	0.72	0.20	0.28	0.05	0.58	0.15	0.42	0.09	IOD_MAM1
IOD_DJF2	0.54	0.10	0.46	0.08	0.69	0.14	0.31	0.06	0.53	0.08	0.47	0.05	IOD_JJA1
IOD_MAM2	0.52	0.09	0.48	0.08	0.52	0.09	0.48	0.07	0.50	0.07	0.50	0.05	IOD_SON1
IOD_JJA2	0.52	0.07	0.48	0.07	0.40	0.05	0.60	0.09	0.61	0.11	0.39	0.04	IOD_DJF2
IOD_SON2	0.47	0.08	0.53	0.09	0.35	0.05	0.65	0.13	0.64	0.17	0.36	0.06	IOD_MAM2
SOI_DJF1	0.54	0.08	0.46	0.06	0.73	0.20	0.27	0.05	0.68	0.12	0.32	0.04	SOI_JJA0
SOI_MAM1	0.58	0.10	0.42	0.07	0.58	0.08	0.42	0.06	0.65	0.12	0.35	0.07	SOI_SON0
SOI_JJA1	0.48	0.08	0.52	0.11	0.25	0.05	0.75	0.31	0.73	0.15	0.27	0.04	SOI_DJF1
SOI_SON1	0.68	0.20	0.32	0.07	0.28	0.06	0.72	0.23	0.54	0.14	0.46	0.12	SOI_MAM1
SOI_DJF2	0.67	0.21	0.33	0.08	0.22	0.06	0.78	0.29	0.46	0.11	0.54	0.11	SOI_JJA1
SOI_MAM2	0.75	0.28	0.25	0.07	0.34	0.07	0.66	0.14	0.57	0.10	0.43	0.08	SOI_SON1
SOI_JJA2	0.66	0.15	0.34	0.06	0.75	0.18	0.25	0.04	0.56	0.09	0.44	0.07	SOI_DJF2
SOI_SON2	0.65	0.13	0.35	0.05	0.67	0.18	0.33	0.06	0.52	0.12	0.48	0.11	SOI_MAM2

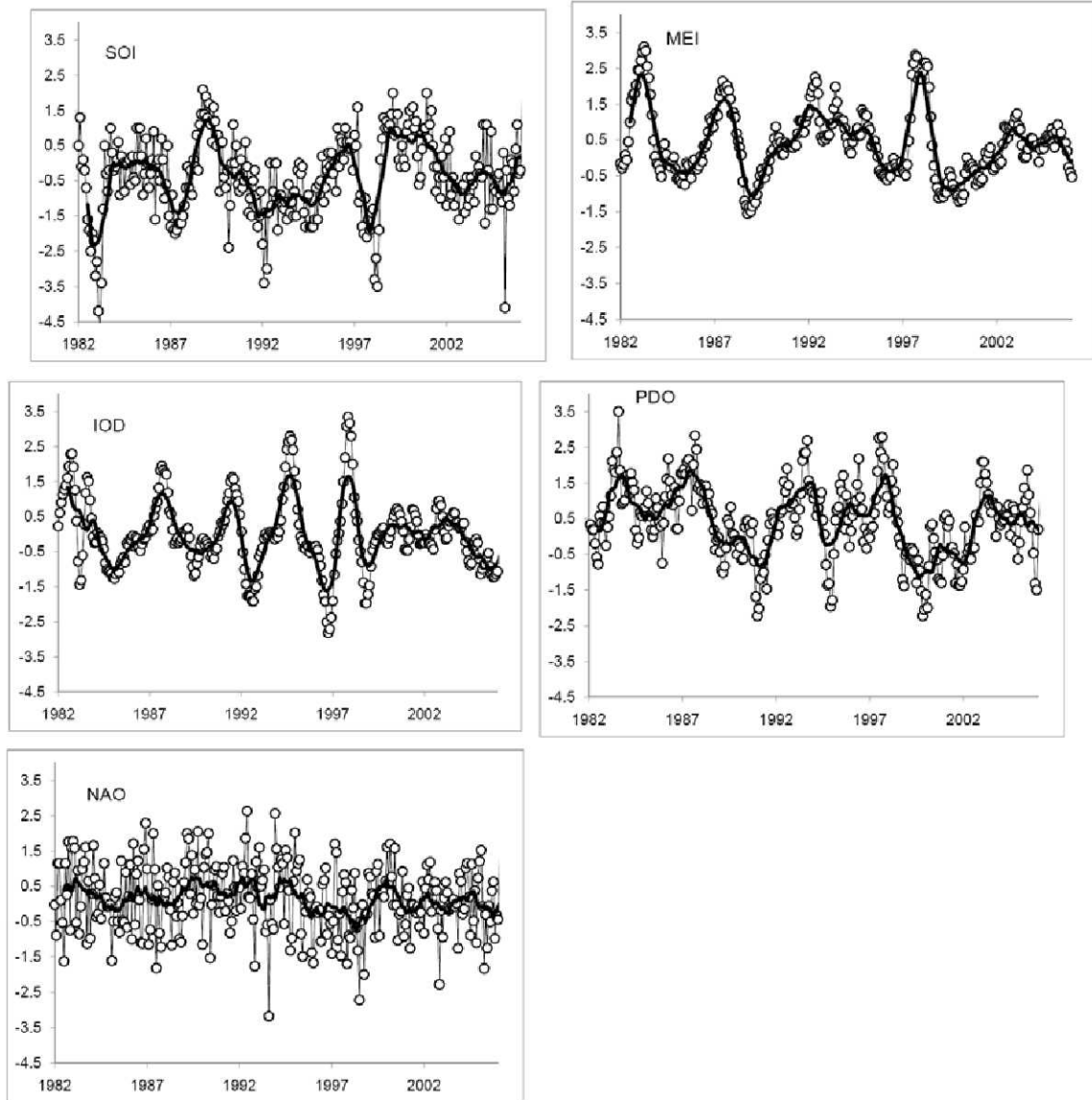


Figure 1. Monthly SOI, MEI, IOD, PDO and NAO indices from 1982-2007 with a 12 month trend line plotted. In this paper, we aggregate the monthly indices into seasonal averages to correlate with phenology metrics.

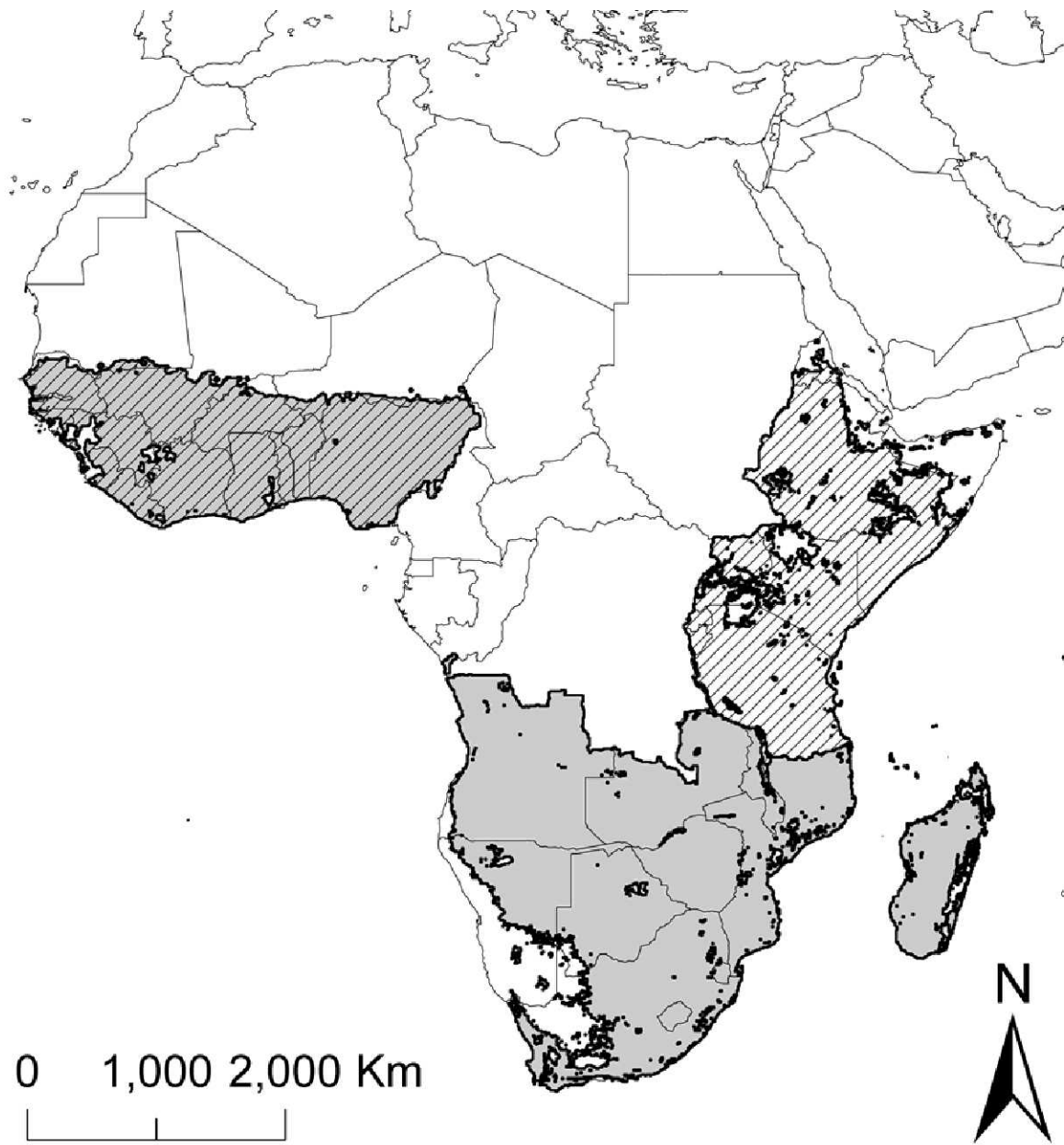


Figure 2. Map with regions addressed in this study. The gaps occur because a mask was applied eliminating all pixels with NDVI <0.2 or >0.7 or where the coefficient of variation of NDVI was <0.1 .

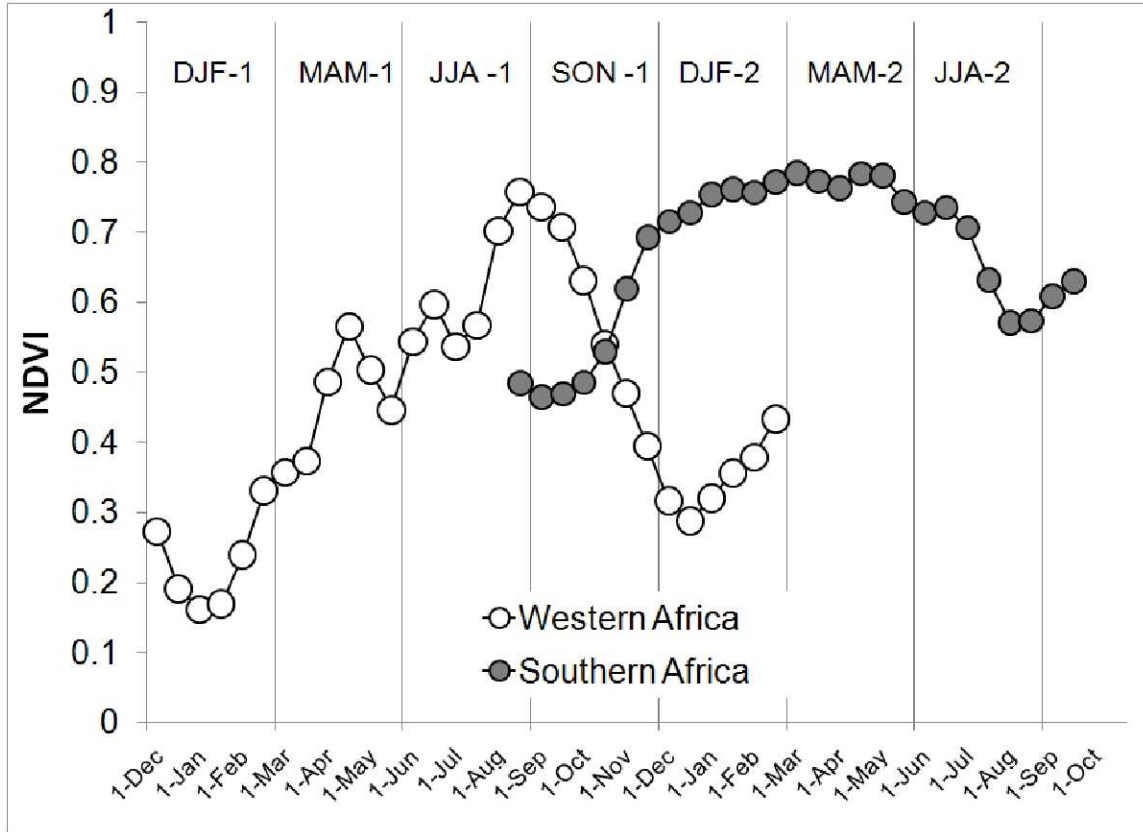


Figure 3. Two NDVI curves from Western and Southern Africa showing the two cycles of analysis, each a year and a half long: Cycle 1: October Year 1 – March Year 3, which captures summer rainy seasons which occur north of the equator, and Cycle 2: April Year 2 – October Year 3, which captures winter rainy seasons, such as are prevalent south of the equator.

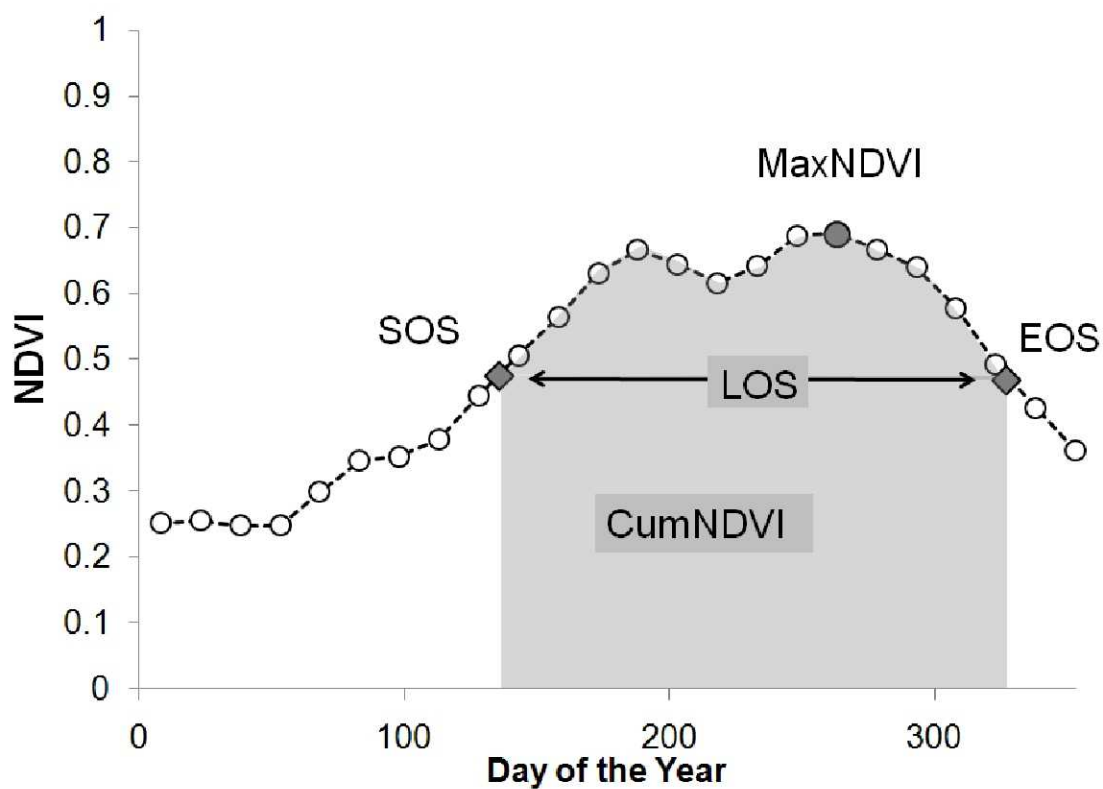
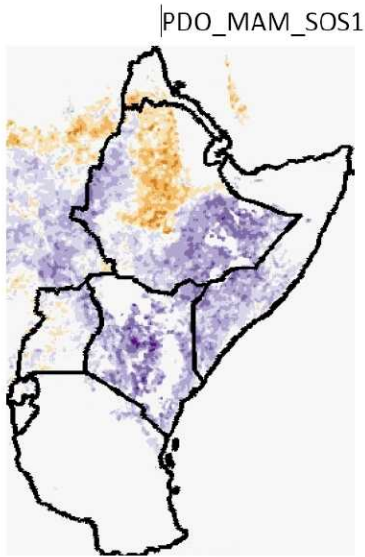


Figure 4. Phenology metrics using the threshold method, indicating the start of season (SOS), length of season (LOS), date of maximum NDVI of the season (maxNDVI), and the cumulated NDVI over the season (cumNDVI).

A.



B.

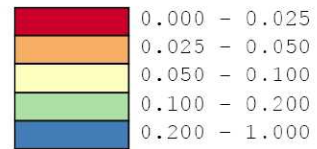
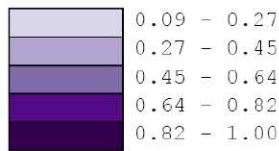
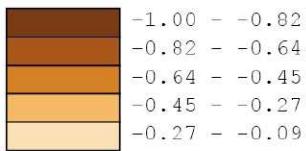
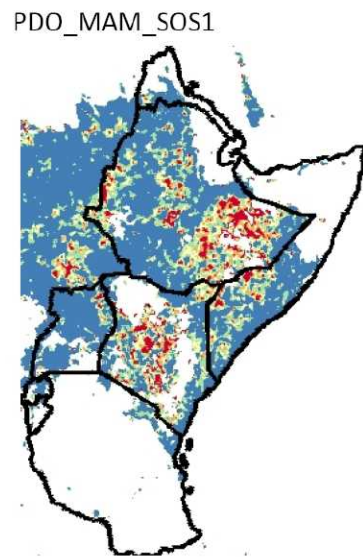


Figure 5. A. Image shows the correlation between the Pacific Decadal Oscillation during the March-April-May period on the start of season metric derived from NDVI from 1981-2007 in Eastern Africa. Note the differential effect in central Ethiopia where the high elevation areas are located. B. shows the significance (p value) of A. Brown colors in A. refer to earlier start times, blue colors to later start times.

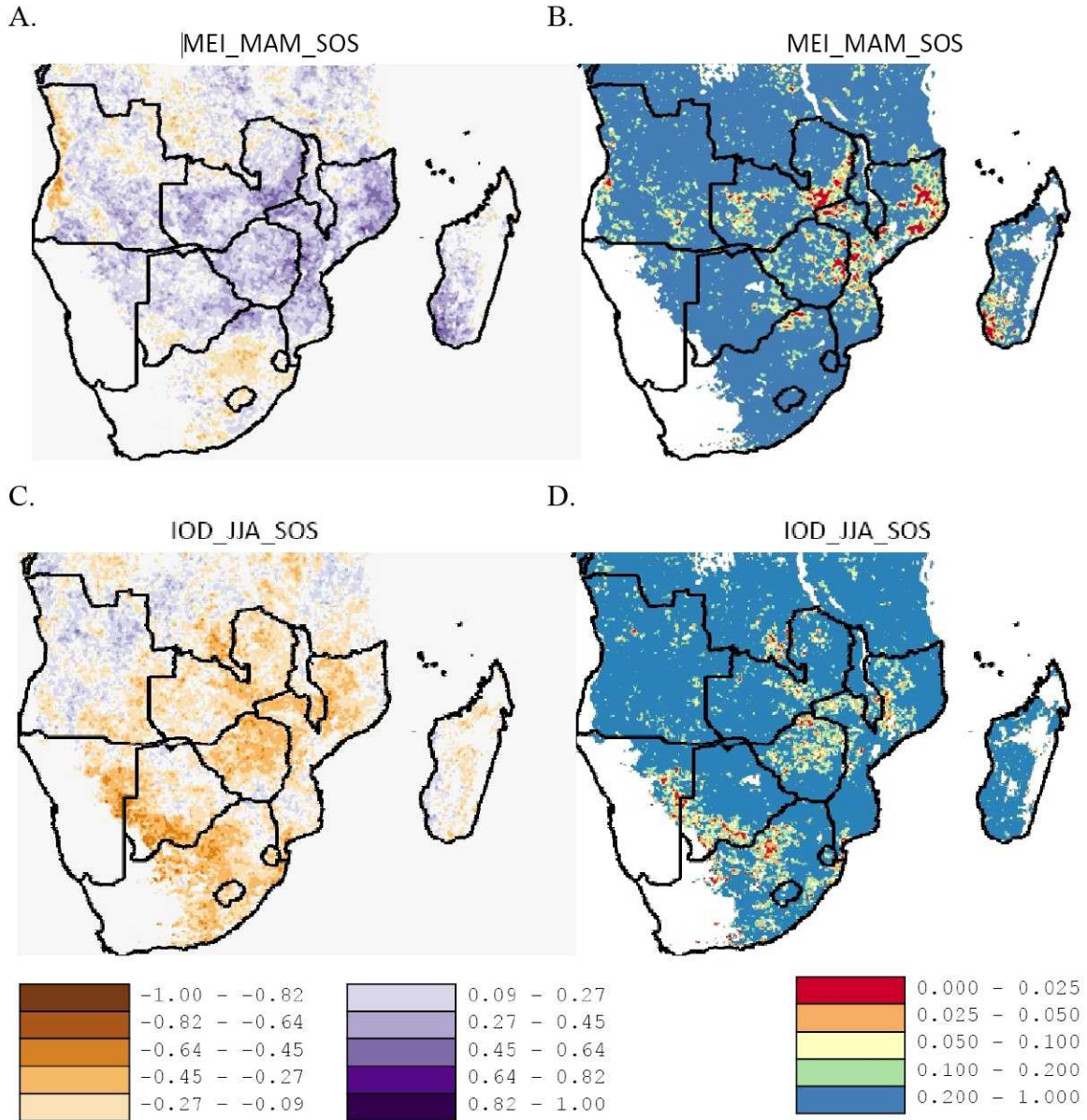
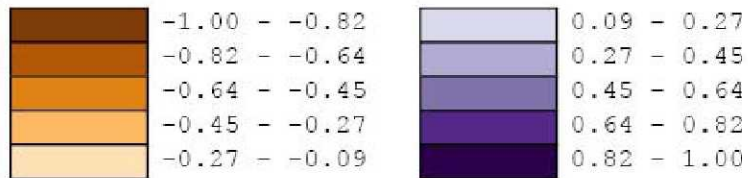
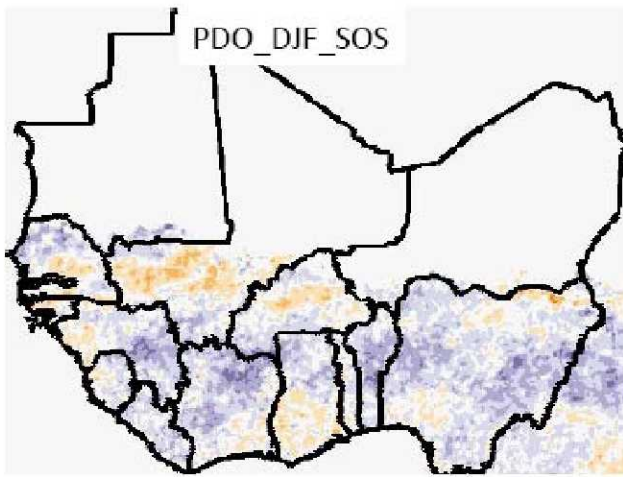


Figure 6. A. Correlation between the MEI from March-April-May (MAM) and start of season (SOS), B. shows the significance (p value) of A, C. Correlation between the IOD from June-July-August (JJA) on SOS in southern Africa, D. Significance of the correlation shown in C. Brown colors in the correlation refer to earlier start times, blue colors to later start times.

A.



B.

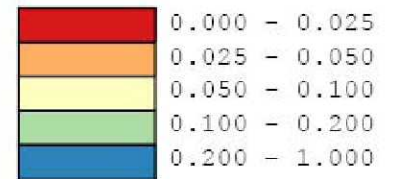
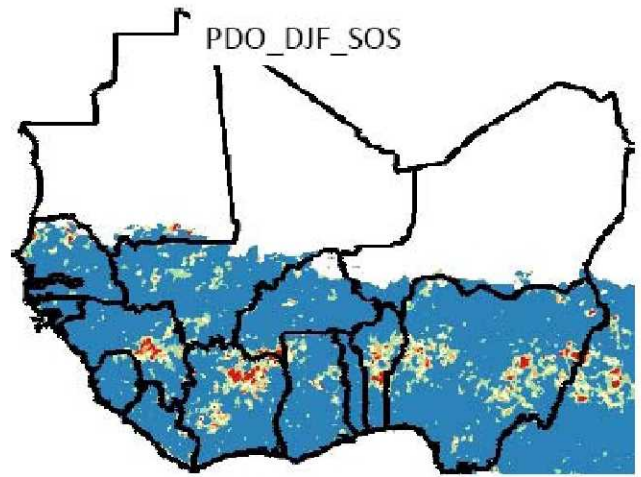


Figure 7. A. Correlation between the PDO from December-January-February (DJF) and start of season, B. shows the significance (p value) of the correlation in Western Africa. Brown colors in A correlate to earlier start times, blue colors to later start times.

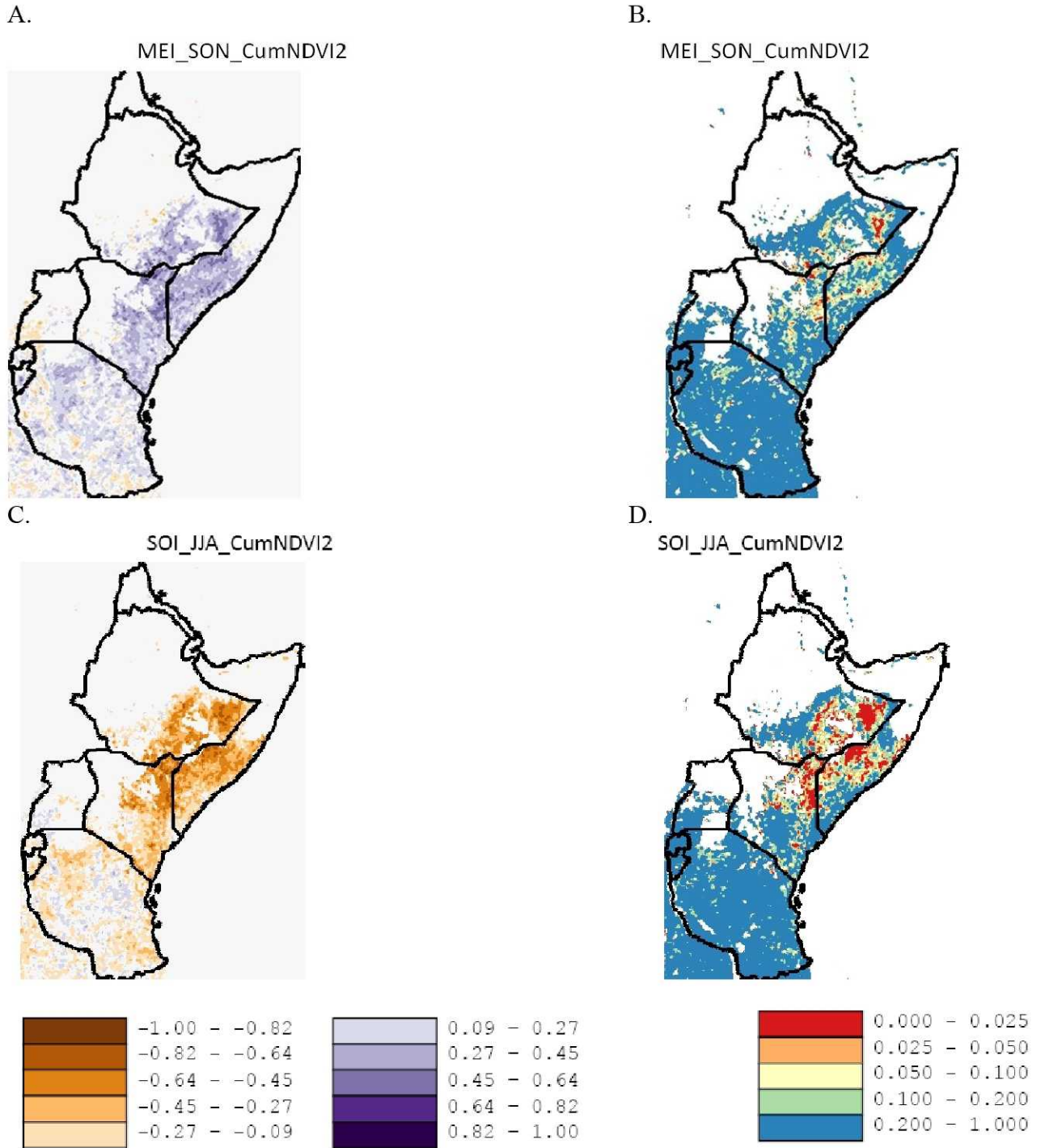


Figure 8. A. Correlation between the MEI from September-October-November and cumulative NDVI, B. shows the significance (p value) of A, C. Correlation between the SOI from June-July-August (JJA) on cumulative NDVI, D. Significance of the correlation shown in C. Brown colors correlate to earlier start times, blue colors to later start times.

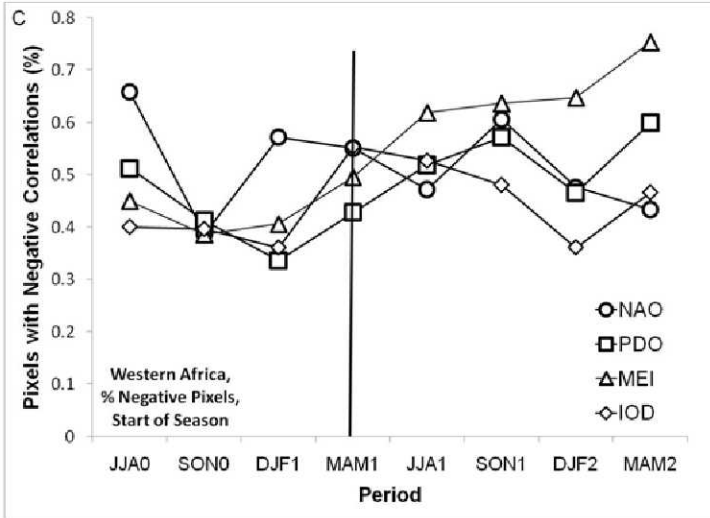
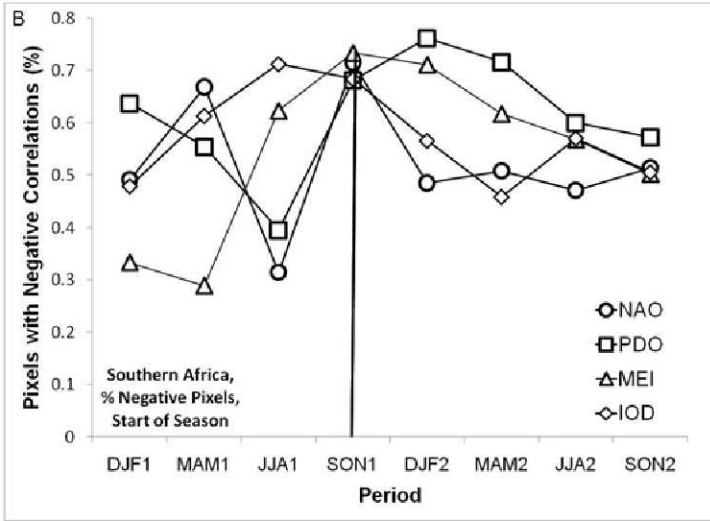
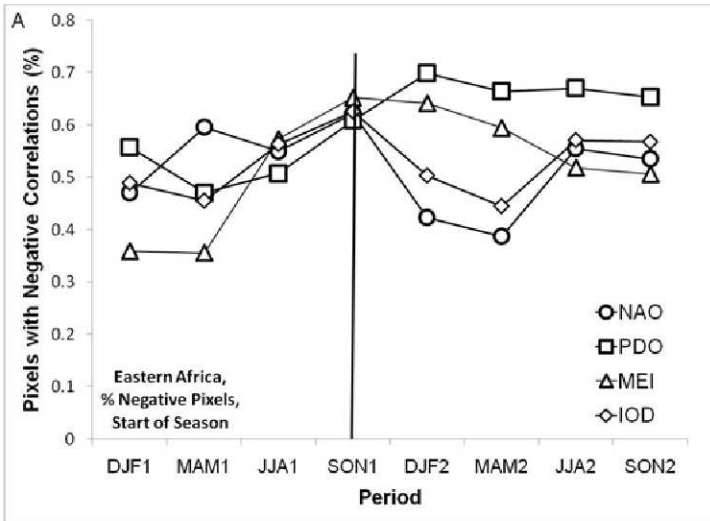


Figure 9. Analysis of the negative impact of four climate indices (NAO, PDO, MEI and IOD) on SOS for the three regions Eastern Africa (A), Southern Africa (B) and Western Africa (C). The black vertical lines correspond to the period when on average SOS occurs

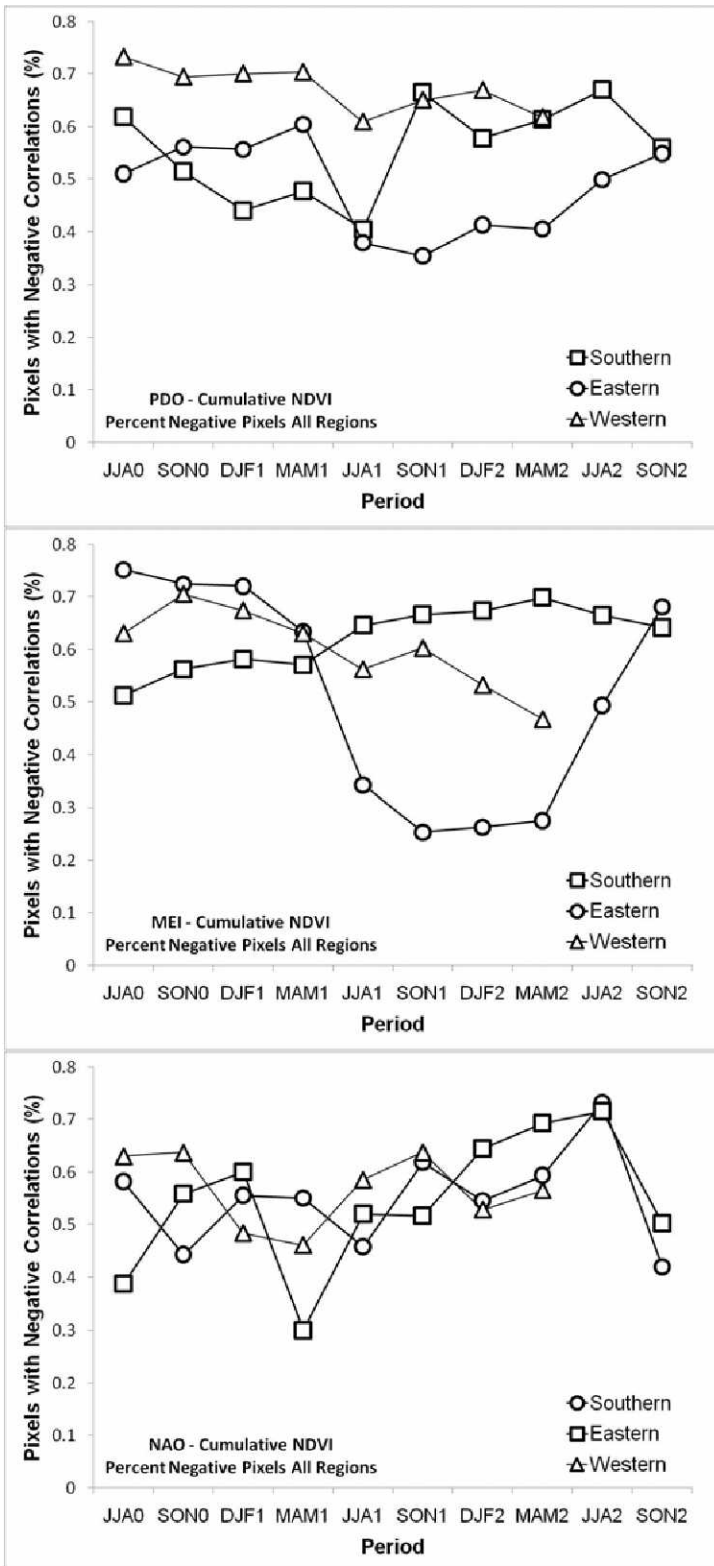


Figure 10. PDO, MEI and NAO effects by percent of region on cumulative NDVI.

References

- Alberts, B., & Mehta, G. (2004). *Realizing the Promise and Potential of African Agriculture*. Amsterdam, The Netherlands: Interacademy Council
- Anyamba, A. (1997). Interannual Variations of NDVI over Africa and their Relationship to ENSO: 1982-1995. In, *Department of Geography* (p. 132): Clark University
- Anyamba, A., Tucker, C.J., & Eastman, J.R. (2001). NDVI anomaly patterns over Africa during the 1997/1998 ENSO warm event. *International Journal of Remote Sensing*, 22, 1847-1859
- Bonan, G. (2002). *Ecological Climatology*. London: Cambridge University Press
- Breman, H. (2003). West Africa's Subsistence Farming. In (p. 16). Togo: Food and Agriculture Organization, Rome
- Brown, M.E. (2008a). *Famine Early Warning Systems and Remote Sensing Data*. Heidelberg: Springer Verlag
- Brown, M.E. (2008b). *Famine Early Warning Systems and Remote Sensing Data*. Heidelberg: Springer Verlag
- Brown, M.E., & De Beurs, K.M. (2008). Evaluation of Multi-Sensor Semi-Arid Crop Season Parameters Based on NDVI and Rainfall. *Remote Sensing of Environment*, 112, 2261-2271
- Brown, M.E., Funk, C., Galu, G., & Choularton, R. (2007). Earlier Famine Warning Possible Using Remote Sensing and Models. *EOS Transactions of the American Geophysical Union*, 88, 381-382
- Brown, M.E., Pinzon, J.E., & Prince, S.D. (2006). The Sensitivity of Millet Prices to Vegetation Dynamics in the Informal Markets of Mali, Burkina Faso and Niger. *Climatic Change*, 78, 181-202
- Cane, M.A., Clement, A., Kaplan, A., Kushnir, Y., Pozdnyakov, D., Seager, R., Zebiak, S.E., & Murtugudde, R. (1996). 20th-Century Sea-Surface Temperature Trends. *Science*, 275, 957-960
- Chen, J., Jönsson, P., Tamura, M., Gu, Z., Matsushita, B., & Eklundh, L. (2004). A simple method for reconstructing a high-quality NDVI time-series data set based on the Savitzky-Golay filter. *Remote Sensing of Environment*, 91, 332-344
- Chen, X.Q., Tan, Z.J., Schwartz, M.D., & Xu, C.X. (2000). Determining the growing season of land vegetation on the basis of plant phenology and satellite data in Northern China. *International Journal of Biometeorology*, 44, 97-101
- Chuvieco, E. (1999). Measuring changes in landscape pattern from satellite images: short-term effects of fire on spatial diversity. *International Journal of Remote Sensing*, 20, 2331-2346
- de Beurs, K.M., & Henebry, G.M. (2008). Northern Annular Mode effects on the Land Surface Phenologies of Northern Eurasia. *Journal of Climate*, 21, 4257-4279

- Eastman, J.R., Anyamba, A., & Ramachandran, M. (1996). The Spatial Manifestations of ENSO Warm Phase Events in Southern Africa. In, *Conference on the Application of Remotely Sensed Data and Geographic Information Systems in Environmental and Natural Resources Assessment in Africa*. Harare, Zimbabwe
- FAO (2006). The State of Food Insecurity in the World. In (p. 30). Rome, Italy: United Nations Food and Agriculture Organization
- FEWS (1992). Determining Start of the Growing Season using Max NDVI. In (p. 18). Arlington, VA: FEWS-ARD
- FEWS (2008). Food Price Database at USGS Africa Data Dissemination Service (ADDS). In: USAID
- FEWSNET (2006). KENYA FOOD SECURITY UPDATE – DECEMBER 6, 2006. In (p. 5). Washington DC: Famine Early Warning System Network
- Fontaine, B., Trzaska, S., & Janicot, S. (1998). Evolution of the Relationship between near Global and Atlantic SST Modes and the Rainy Season in West Africa: Statistical Analyses and Sensitivity Experiments. *Climate Dynamics*, 14, 353-368
- Funk, C., & Budde, M. (2008). Phenologically-tuned MODIS NDVI-based production anomaly estimates for Zimbabwe. *Remote Sensing of Environment*, *accepted*
- Funk, C., Dettinger, M.D., Michaelsen, J.C., Verdin, J.P., Brown, M.E., Barlow, M., & Hoell, A. (2008). Warming of the Indian Ocean threatens eastern and southern African food security but could be mitigated by agricultural development. *Proceedings of the National Academy of Science*, 105, 11081-11086
- Funk, C., Sanay, G., Asfaw, A., Korecha, D., Choularton, R., Verdin, J., Eilerts, G., & Michaelsen, J. (2005). Recent Drought Tendencies in Ethiopia and Equatorial-Subtropical Eastern Africa. In (p. 11). Washington DC: Famine Early Warning System Network, USAID
- Glantz, M.H., Katz, R.W., & Nicholls, N. (1991). *Teleconnections Linking World Wide Climate Anomalies: Scientific Basis and Societal Impact*. New York: Cambridge University Press
- Green, R.M., & Hay, S.I. (2002). The potential of Pathfinder AVHRR data for providing surrogate climatic variables across Africa and Europe for epidemiological applications. *Remote Sensing of Environment*, 79, 166-175
- Groten, S.M.E., & Ocatre, R. (2002). Monitoring the length of the growing season with NOAA. *International Journal of Remote Sensing*, 24, 2797-2815
- Holben, B. (1986). Characteristics of Maximum-Value Composite Images from Temporal AVHRR Data. *International Journal of Remote Sensing*, 7, 1417-1434
- Hurrell, J.W. (1995). Decadal trends in the North Atlantic Oscillation: Regional temperatures and precipitation. *Science*, 269, 676-679

- Ji, L., & Peters, A.J. (2003). Assessing vegetation response to drought in the northern Great Plains using vegetation and drought indices. *Remote Sensing of Environment*, 87, 85-98
- Jones, P.D., Jónsson, T., & Wheeler, D. (1997). Extension to the North Atlantic Oscillation using early instrumental pressure observations from Gibraltar and South-West Iceland. *International Journal of Climatology*, 17, 1433-1450
- Jury, M.R., McQueen, C., & Levey, K. (1994). SO1 and QBO Signals in the African Region. *Theoretical and Applied Climatology*, 50, 103-115
- Lehman, E.L., & D'Abbrera, H.J.M. (1975). *Nonpara-metrics-Statistical Methods Based on Ranks*. San Francisco,CA: Holden-Day
- Mabaso, M., Kleinschmidt, I., Sharp, B., & Smith, T. (2009). El Niño Southern Oscillation (ENSO) and annual malaria incidence in Southern Africa. *Transactions of the Royal Society of Tropical Medicine and Hygiene*, 101, 326-330
- Mantua, N.J., Hare, S.R., Zhang, Y., Wallace, J.M., & Francis, R.C. (1997). A Pacific interdecadal climate oscillation with impacts on salmon production. *Bulletin of the American Meteorological Society*, 78, 1069-1079
- Nicholson, S. (2003). The South Indian Convergence Zone and Interannual Rainfall Variability over Southern Africa and the Question of ENSO's Influence on Southern Africa. *Journal of Climate*, 16, 555-562
- Parry, M.L., Canziani, O.F., Palutikof, J.P., Linden, P.J.v.d., & Hanson, C.E. (Eds.) (2007). *IPCC, 2007: Climate Change 2007: Impacts, Adaptation and Vulnerability. Contribution of Working Group II to the Fourth Assessment Report of the Intergovernmental Panel on Climate Change*. Cambridge, UK: Cambridge University Press
- Pinzon, J., Brown, M.E., & Tucker, C.J. (2005). Satellite time series correction of orbital drift artifacts using empirical mode decomposition. In N. Huang (Ed.), *Hilbert-Huang Transform: Introduction and Applications* (pp. 167-186)
- Rasmussen, E. (1991). Observational aspects of ENSO cycle teleconnections. In R.W.K. M. H. Glantz, and N. Nicholls (Ed.), *Teleconnections Linking Worldwide Climate Anomalies* (pp. 309-344): Cambridge University Press
- Rasmussen, M.S. (1998). Developing simple, operational, consistent NDVI-vegetation models by applying environmental and climatic information. Part I: Assessment of net primary production. *International Journal of Remote Sensing*, 19, 97-119
- Rasmusson, E.M., & Wallace, J.M. (1983). Meteorological aspects of the El Niño/Southern Oscillation. *Science*, 222, 1195-1202
- Reason, C.J.C., & Rouault, M. (2002). ENSO-like decadal variability and South African rainfall. *Geophysical Research Letters*, 29, 10.1029/2002GL014663, 014616-014661-014664
- Reynolds, R.W., Rayner, N.A., Smith, T.M., Stokes, D.C., & Wang, W. (2002). An Improved In Situ and Satellite SST Analysis for Climate. *Journal of Climate*, 15, 1609-1625

- Ropelewski, C.F., & Halpert, M.S. (1986). Global and Regional Scale Precipitation Patterns Associated with the El Nino/Southern Oscillation. *Monthly Weather Review*, *115*, 1606-1626
- Ropelewski, C.F., & Halpert, M.S. (1987). Global and Regional Scale Precipitation Patterns Associated with the El Nino/Southern Oscillation. *Monthly Weather Review*, *115*, 1606-1626
- Saji, N., Goswami, B., & Yamagata, T. (1999). A dipole mode in the tropical Indian Ocean. *Nature*, *401*, 360-363
- Thompson, D.W., & Wallace, J.M. (2001). Regional climate impacts of the Northern Hemisphere Annular Mode. *Science*, *293*, 85-89
- Tucker, C.J., Pinzon, J.E., Brown, M.E., Slayback, D., Pak, E.W., Mahoney, R., Vermote, E., & Saleous, N. (2005). An Extended AVHRR 8-km NDVI Data Set Compatible with MODIS and SPOT Vegetation NDVI Data. *International Journal of Remote Sensing*, *26*, 4485-4498
- UCAR (2009). Persistent Patterns that Shape Weather and Climate Variability—A Glossary. In B.H. Kevin Trenberth, Zhenya Gallon (Ed.), *Backgrounders*. Boulder, CO: NCAR/UCAR
- USAID (2007). The History of America's Food Aid. In: US State Department
- Vasagar, J. (2005). Plenty of Food - Yet the Poor are Starving. In, *Guardian (UK)*. TAHOUA, Niger
- Verdin, J., Funk, C., Kalver, R., & Roberts, D. (1999). Exploring the correlation between Southern Africa NDVI and Pacific sea surface temperatures: results for the 1998 Maize growing season. *International Journal of Remote Sensing*, *20*, 2117-2124
- Verdin, J., Lietzow, R., Rowland, J., Klaver, R., Reed, B., French, V., & Lee, F. (2000). A Comparison Of Methods For Estimating Start-Of-Season From Operational Remote Sensing Products: First Results. In (p. 13). Sioux Falls, SD: USGS-EROS Data Center
- Vrieling, A., De Beurs, K.M., & Brown, M.E. (2008). Recent trends in agricultural production of Africa based on AVHRR NDVI time series. In, *SPIE Europe Security + Defense*. Cardiff, UK
- Wang, G. (2003). Reassessing the impact of North Atlantic Oscillation on the sub-Saharan vegetation production. *Global Change Biology*, *9*, 493-499
- White, M.A., Thornton, P.E., & Running, S.W. (1997). A continental phenology model for monitoring vegetation responses to interannual climatic variability. *Global Biogeochemical Cycles*, *11*, 217-234
- Wolter, K., & Timlin, M.S. (1998). Measuring the strength of ENSO - how does 1997/98 rank? *Weather*, *53*, 315-324
- Zhang, R., & Delworth, T.L. (2006). Impact of Atlantic multidecadal oscillations on India/Sahel rainfall and Atlantic hurricanes. *Geophysical Research Letters*, *33*, doi:10.1029/2006GL026267

